

Review

Carbons as Catalysts in Thermo-Catalytic Hydrocarbon Decomposition: A Review

Randy Vander Wal * and Mpila Makiessie Nkiawete

The EMS Energy Institute and the John and Willie Leone Family Department of Energy and Mineral Engineering, The Pennsylvania State University, University Park, PA 16802, USA; mmn19@psu.edu

* Correspondence: ruv12@psu.edu

Received: 25 February 2020; Accepted: 9 April 2020; Published: 14 April 2020



Abstract: Thermo-catalytic decomposition is well-suited for the generation of hydrogen from natural gas. In a decarbonization process for fossil fuel—pre-combustion—solid carbon is produced, with potential commercial uses including energy storage. Metal catalysts have the disadvantages of coking and deactivation, whereas carbon materials as catalysts offer resistance to deactivation and poisoning. Many forms of carbon have been tested with varied characterization techniques providing insights into the catalyzed carbon deposition. The breadth of studies testing carbon materials motivated this review. Thermocatalytic decomposition (TCD) rates and active duration vary widely across carbons tested. Regeneration remains rarely investigated but does appear necessary in a cyclic TCD–partial oxidation sequence. Presently, studies making fundamental connections between active sites and deposit nanostructures are few.

Keywords: thermo-catalytic decomposition; hydrogen; natural gas; carbon catalyst

1. Introduction

Sustainability of Thermo-Catalytic Decomposition of Methane and Natural Gas Components

Hydrogen is envisioned as the energy carrier (fuel) of the future and is a crucial feedstock for various manufacturing industries. Presently, 55 million metric tons (MMT) are produced annually; 98% of this is from reforming fossil fuels, for use in oil refineries, methanol production and ammonia production [1]. Steam reforming of methane (SMR), the present industrial practice, produces 13.7 kg CO₂ (equiv.)/kg of net hydrogen [2] and consumes 19.8 L of water per kg of hydrogen [3]. Thermo-catalytic decomposition of methane is an attractive alternative to conventional steam reforming because the process does not generate CO/CO₂ byproducts or consume water resources, so the needs for water–gas shift and CO₂ removal stages, along with stock desulphurization and steam generation are eliminated. The energy requirement for methane cracking process (37.8 kJ/mole of H₂) is less than that for steam reforming (75.6 kJ/mole of CH₄) [1,4].

The article begins with the motivating factors for TCD, followed by a description of deposited carbon characterization—for structure via XRD, XPS, Raman and texture. Across studies, differences are observed over time as carbon deposition continues—signaling both differences between the depositing carbon and the original carbon catalyst, but more importantly, an evolution of the depositing carbon structure. This bears implications for longevity of TCD operation and timing for interleaved regeneration processes. Notably, few studies have utilized TEM for analysis of the deposited carbon nanostructure—though it would provide insights into the depositing carbon nanostructure. Results with other natural gas components or mixtures are sorely absent despite being the feedstock for TCD at scale. The article concludes with directions for fundamental studies critical to the mechanistic understanding of TCD and catalyst activity.

Thermo-catalytic decomposition (TCD) of methane can produce CO_x-free hydrogen for PEM fuel cells, oil refineries, ammonia and methanol production [5]. Recent research has focused on enhancing the production of hydrogen by the direct thermo-catalytic decomposition of methane to form elemental carbon and hydrogen as an attractive alternative to the conventional steam reforming process [6]. Hybrid solar-fossil thermochemical processes that make use of an external source of concentrated solar radiation for supplying process heat, offer viable and efficient routes for fossil fuel decarbonization and CO₂ sequestration. It prepares the path to the hydrogen economy, as it represents a mid-term transition from fossil fuel to renewable hydrogen energy systems [7]. As an example, using a solar reactor, Abanades et al. demonstrated CH₄ conversion and H₂ yield exceeding 97% and 90%, respectively, but catalyst deactivation occurred progressively because of carbon deposition on the carbon catalyst [8]. Direct solar and wind can similarly provide the energy for TCD, effectively storing renewable energy in the (desirable) form of chemical bond energy; i.e., H₂. These features of TCD are illustrated in Figure 1. Yet kinetic modeling in reactors is presently limited by a poor understanding of the deactivation of the carbon catalysts [9].

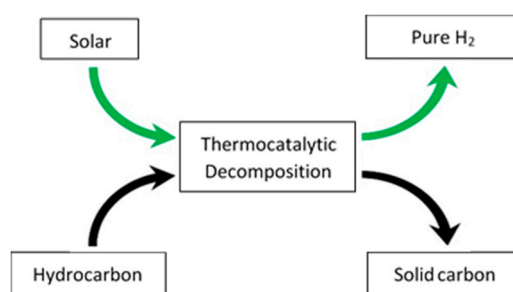


Figure 1. Inputs and outputs of TCD.

TCD is a clean technology. Life-cycle assessments [10] and techno-economic analyses [11–13] are positive [14–16]. Non-catalytic decomposition requires temperatures of ≈ 1200 °C, whereas with a catalyst, as in TCD, decomposition can be accomplished in the range 850–900 °C [6]. Metal catalysts have been studied, but invariably they deactivate [1,6,9]. Their regeneration requires carbon (deposit) burn-off, negating carbon capture benefits [2,3,5,10,14], and ultimately limiting their life [15,16]. Carbon as a catalyst has many advantages compared to other catalytic materials: (a) fuel flexibility, (b) insensitivity to sulfur poisoning, (c) high temperature resistance and (d) selectable surface area and porosity dependent upon carbon type. The process not only offers convenient carbon capture as an environmentally benign solid, but offers multiple commercial uses as electrode material, carbon adsorbents or for soil beneficiation [17]. Despite these advantages, carbon as a catalyst also problematically deactivates. Ideally, the deposited carbon would be autocatalytic, but all studies with methane find that *the deposited carbon is not as active a catalyst as the original carbon*.

In summary, TCD offers the following technical and societal benefits.

1. Decarbonizing a fossil fuel for clean H₂, providing a bridge to the H₂ economy;
2. Enabling renewable energy coupling/storage into chemical bond energy;
3. Producing solid carbons as energy storage media, for potential structural materials and realizing at-scale solid carbon sequestration.

The chief technological barrier is the present inability to maintain long-term TCD activity. The fundamental research needed is to understand the origin of carbon catalyst deactivation towards its prevention or by its renewal through regeneration.

2. Thermo-Catalytic (Methane) Decomposition—Literature Analysis

2.1. Deposition

Various TCD systems have included fixed [18,19] and fluidized beds [20–23], pilot-scale reactors [24] and laboratory gravimetric instruments [25]. Most studies have been conducted with activated carbons [19,26–29], carbon blacks [30–32] or both [21,33,34]. Activated carbons with large initial surface areas rapidly deactivate, whereas carbon blacks with small surface areas deactivate very slowly. Yet other studies using coal char were conducted to improve the process economics [35,36].

During the methane TCD process, the catalyst deactivates due to intensive carbon deposition, as shown in Figure 2. The dependencies of TCD rate upon initial carbon catalyst and non-monotonic variations with continued reaction/deposition are illustrated in the rate plot from Suelves et al., as shown in Figure 2; the figure shows non-monotonic rates with time, and very different rate behaviors between the different carbon catalysts [34]. Muradov et al. studied several forms of carbons (e.g., carbon blacks (CBs), activated carbons (ACs) and graphites) and found that more disordered forms of carbon are more active than ordered ones; the order of catalytic activity correlating with structure: amorphous > turbostratic > graphitic [21]. Ultimately the deposit has less surface area and activity compared to the original carbon catalyst, and its activity is influenced by its structure ranging from amorphous to crystalline depending upon how the deposited carbon is formed.

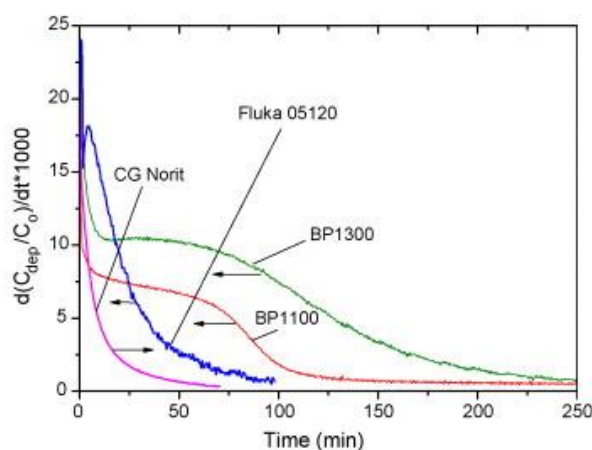


Figure 2. Decline in deposition rate (normalized to initial carbon mass), and variability for different carbon blacks (BP1300, BP1100, Fluka 05120), and an activated carbon (CG Norit) [34].

The changing structure of the deposited carbon was best illustrated by Lazaro et al., who reported XRD profiles of the catalyst with deposit as the run progressed, shown in Figure 3 [37]. Although the carbon black had a highly disordered structure, a marked increase in order was observed, as gauged by sharpness of the (002) peak at 26° and emergence of the (101) peak at $\approx 78^\circ$ [37]. Furthermore, the $d_{(002)}$ spacing decreased linearly from 0.385 nm for fresh catalyst down to 0.345 nm for the deactivated catalyst. Based on these values, the authors concluded that the deposited carbon was more graphitic than the fresh catalyst. This study strongly supports deactivation as being due to a change in structure, with that structure evolving over time, and ultimately being quite different than that of the initial carbon. Notably a key advantage of carbon blacks is their comparative lack of porosity compared to ACs, and hence lesser susceptibility to pore blockage, contributing to declining activity, allowing a clearer insight into the operative mechanism(s) governing a declining rate.

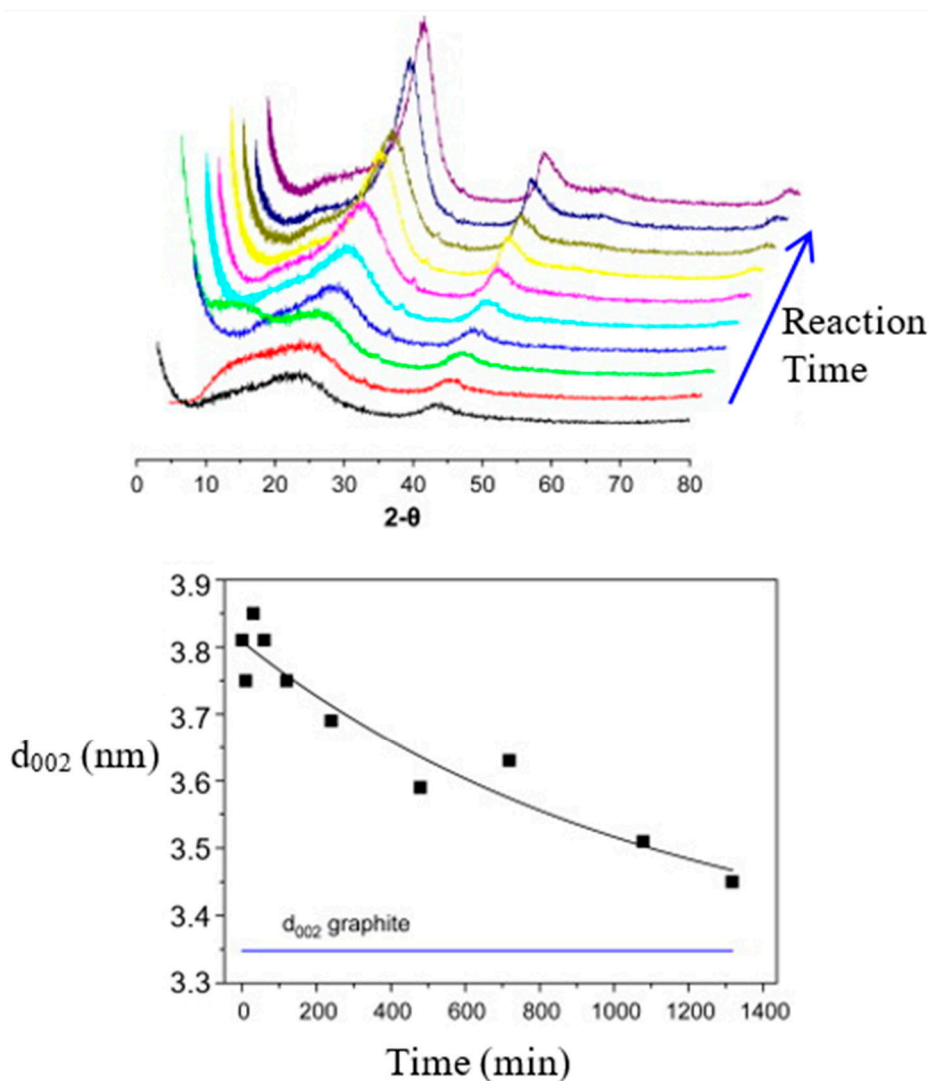


Figure 3. Change of the XRD pattern with reaction time (top) and extracted $d_{(002)}$ value (bottom) during the test at 950 °C, carbon black as catalyst [37].

Although Lazaro et al. found *initial* activity to depend upon surface oxygen groups [37], the consensus is that activity does not depend nor correlate to oxygen content, consistent with the fact that these groups are rapidly removed during the reaction. Several groups have investigated the correlation between surface area and activity/rate; no correspondence has been found [21,38,39]. In comparing the catalytic activity of virgin AC (lignite) with that pre-treated with pure hydrogen at 850 °C to remove oxygen groups, Muradov et al. [21] showed that beyond the initial stage, catalytic activity was not dependent upon such groups. Similarly, Moliner et al. attributed the short-term rate to (surface) oxygen groups, but capacity (and hence overall rate) showed no correlation to oxygen content [28]; Pinilla et al. did the same [40]. Meanwhile in extensive studies of activated carbons, Kim et al. found no relation of capacity to surface area [27].

While Lazaro et al. showed the $d_{(002)}$ parameter to decrease linearly with time [37], Dunker et al. concluded crystallites were not generally responsible for deactivation, using XRD and the $d_{(002)}$ as a descriptor for the degree of graphitic structure [23]. By comparison to carbon blacks, Muradov et al. found high catalytic activity of plasma-generated carbons for methane decomposition. These authors attributed this to the increased surface concentration of high-energy sites formed during non-equilibrium, plasma-assisted dissociation of a carbon precursor [41]. In contrast, XRD measurements reported by Lazaro in Figure 3 show increasing order in the depositing carbon, as

measured by the decreasing $d_{(002)}$ value with time [37]. Yet Moliner et al. [42] reported that Raman and XRD revealed no difference between deposit and catalyst (coal char). Similarly, Suelves et al. also stated that XRD results revealed no substantial structural changes between fresh and used samples, suggesting that the deactivation mechanism cannot be associated with differential structural changes, but rather, loss of surface area [32,34]. Conversely, by applying XRD and temperature programmed oxidation (TPO) to fresh versus deactivated catalyst, Pinilla et al. showed the deposit to be markedly more graphitic, based on differences in (002) peak width and oxidation temperature [43]. Additionally, Serrano et al. found different activities between CBs to be consistent with their quite different XRD intensity ratios C(101)/C(002) of 0.95 and 0.64 [44]. In subsequent studies using XPS, those authors found a direct relationship between the number of defects and threshold TCD temperature, as a measure of activity [45]. Defects, whether in the form of vacancies disrupting sp^2 network or topological defects distorting the binding energy, broaden the FWHM (full width at half maximum) of the C 1s peak. This is consistent with different carbons having different activities reflecting their structures. Additionally, no definitive relation was found between threshold temperature and parameters such as surface area and oxygen group concentration.

Suffice to say, there is disagreement with regard to structure, but such measures include both original carbon and deposition; hence, interpretation is not straightforward. Nevertheless, there is convergence as to the importance of active sites, reflective of underlying structure, and not surface area [27,46]. For example, Muradov et al. attributed different activities of different carbons to differences in surface defects (dislocations, vacancies, discontinuities, etc. [21]), as was also suggested by Kim et al. [27]. Additionally, Lee et al. tested the catalytic characteristics of various carbon blacks [47], finding that the TCD rates across these CBs did not scale with surface area, suggesting other factor(s). Interpreting these results, Malaika concluded that the carbon deposit structure may depend upon the nature of the original catalyst [48].

In support of this, Kameya and Hanamura evaluated the carbon deposited on CB as a potential product [49]. They proposed a correlation between the variation in the catalytic activity and the textural properties. These authors attributed the favorable catalytic characteristics of CB to its microstructure, wherein it possesses many active sites consisting of edges and defects in nano-sized graphitic sheets [49]. Variation in activity over time was attributed to variation in crystallite (lamellae) size, and hence edge site concentration, as inferred by Raman analysis. By analogy, the correlation between surface properties and reactivity has been observed in studies on the oxidation of soot, whose highly disordered microstructure is similar to that of CB. The oxidation behavior of soot has been well described with respect to its surface microstructure [50–53]. With reference to initial carbon catalyst cost, carbon blacks vary widely in price, depending upon the particular grade, the lowest being for so-called rubber blacks and the highest being for conductive carbon blacks. Presently, no study has definitively compared carbon blacks across commercial grades or as being dependent upon their nanostructures.

Muradov et al. proposed that on the surface of disordered carbon, the regular array of carbon bonds is disrupted, forming “free” valences and discontinuities (i.e., the edges and corners of crystallites). The concentration of these sites increases with the decrease in carbon crystallite size, and vice versa (decreases as the carbon becomes more ordered; e.g., during graphitization) [21]. Hence, less ordered carbons have smaller crystallites, and hence more edge sites; the opposite is the case for an ordered, graphitic carbon. Aligning with Malaika, Pinnilla surmised the potential for the initial carbon structure to influence that of the depositing carbon—thereby presenting a “memory” effect, noting that such potential could occur via regeneration as well [43].

In other TCD studies, XRD analysis of the carbon produced from ethylene indicated a turbostratic structure. Moreover, the crystallite size was smaller than that formed from methane or propane, correlating with the higher activity from the carbon it produced. In fact, plotting the relative catalytic activity of deposited carbons produced from ethylene, acetylene, benzene and methane decomposition (normalized against the activity of the carbon from methane) as a function of carbon crystallite size showed that a correlation exists between catalytic activity and crystallite size; i.e., smaller crystallites

correlated with higher activity. This explained the accelerating effect of carbons produced from ethylene, benzene or acetylene on methane decomposition rate in studies by Malaika et al. [48].

2.2. Continued Studies Using Porous or Activated Carbons

Recent studies continue to test porous carbons for their activities and longevities in TCD, presumably for their high surface areas and potential activities. Particular advantages of activated carbons are their availability at industrial scale and comparatively low cost.

Liu et al. compared the catalytic performance of AC and carbon black (CB) catalysts, finding that they exhibited opposite deactivation behaviors with time. Initially, AC showed higher activity, but it deactivated quickly. Though the catalytic activity of CB was low, its activity not only could be maintained, but it also showed an increase. Notably, the deposited carbons were different in shape, orientation and chemical structure—thereby underscoring the importance of the deposited carbon structure to continuing deposition [54]. Mahmoudi et al. evaluated activated carbons based on olive stones as catalysts during hydrogen production by thermocatalytic decomposition of methane. The catalysts showed a high initial activity followed by a rapid drop wherein textural analyses showed that methane decomposition occurred mainly in micropores. Meanwhile, XRD and Raman characterization showed that activated carbons tend to be more organized after reaction [55]. Wang et al. studied coal derived activated carbons with varied mesoporous surface areas ranging from 480 m²/g to 1119 m²/g—correlating with increased activity [56]. An interesting observation was the formation of carbon fiber over the AC surface. In the study by Nishii et al., methane decomposition was carried out on carbons with several different structures (activated carbon (AC), carbon black (CB), meso-porous carbon (MC) and carbon nanofiber (CNF)). They found that the carbon produced by methane decomposition decreases activity by covering the catalyst, but itself also acts as a catalyst irrespective of the original carbon catalysts. Moreover, all of the catalysts continued to maintain a methane conversion ratio of about 17% by catalyzing the produced carbon even after the activity was lowered [57]. *Though implicit in nearly all TCD studies, few ever note or distinguish the contribution of the deposited carbon to continued TCD activity.*

Wieckowski et al. examined methane decomposition on activated carbons across temperatures from 1023 to 1123 K, with the highest conversion observed at 1123 K as 26%. Nevertheless, pores of the catalyst became blocked by the carbonaceous deposit and the methane conversion decreased [58]. Ghani et al. compared five types of activated carbons; they were derived from hardwood, rubber black, coconut shell, coal and graphite using a fixed bed, quartz flow reactor. They found a reaction order of 1 for methane decomposition over the most active catalyst with activation energies ranging from 128 to 205 kJ mol⁻¹ across the carbons [59]. Shen and Lua tested an interconnected trimodal porous carbon (produced by nanocasting) as a catalyst for TCD. With high surface area and large pore volume, the carbon catalyst exhibited high methane conversion and hydrogen yield but further longevity, and conditions were not reported. Presumably, the mesoporosity should increase longevity prior to loss by deposited carbon [60]. Shilapuram and Ozalp utilized thermogravimetry to study hydrogen production by carbon-catalyzed methane decomposition, varying reaction temperature, methane concentration and carbon catalyst. Characteristic deactivation was observed with post-reaction analysis by XRD and SEM, revealing a decreasing disorder with reaction extent and temperature. The expediency of gravimetry should not be overlooked, but a cautionary note is that most thermo-gravimetric analysis (TGA) instruments are not “sealed,” meaning they are not approved for use with “reactive gases.” For TGAs this term refers to flammable or corrosive gases. For reference, the flammability of H₂ in air is ≈4% (v/v), while for methane it is 8% (v/v) [61]. However, commercially sold TGAs are available that are designed for such uses—permitting reaction-order investigations by their capabilities at higher concentrations. Luo et al. found coal-derived ACs to be viable for TCD—with mesoporosity beneficial to catalyst activity and stability [62]. They further note that reduction of oxygen functional groups contribute to the formation of fibrous carbon on the AC surface—illustrating the need for comprehensive catalyst characterization to disentangle catalyst from deposit evolution.

2.3. Novel Studies

Wang et al. investigated the effect of hydrogen addition on methane's decomposition to hydrogen and carbon over an activated carbon catalyst. Their results showed that the addition of H_2 to CH_4 changes both methane conversion over AC and the properties of carbon deposits produced from methane decomposition. Notably, the catalyst's activity was improved, while deactivation lessened by the introduction of H_2 to CH_4 . These results were attributed to a slower loss of pore volume and related surface area [63]. The significance of this study is two-fold. First, it breaks the convention of using bottled methane as a surrogate for natural gas, and second, tests the reactive gas environment for effects upon the depositing carbon structure and associated activity. Indeed, with hydrogen being generated, a small fraction could easily be recycled through the reactor.

Gadkari et al. conducted a numerical analysis of the microwave-assisted thermocatalytic decomposition of methane. Using a 3D mathematical model for microwave-assisted TCD of CH_4 , they developed a simple kinetic model for CH_4 conversion, including catalyst deactivation. Linear variation of CH_4 and H_2 concentration was predicted with good agreement between predicted CH_4 conversion and experimental data. Kinetic model development for heterogeneous catalysis is challenging, particularly when the catalyst itself is evolving, but it is necessary for scaleup [64].

Highlighting the importance of carbon form and structure, Abanades et al. conducted a kinetic investigation of carbon-catalyzed methane decomposition in a thermogravimetric solar gravimetric reactor. Expectedly, the activated carbon showed high initial catalytic activity followed by fast deactivation, whereas the carbon black powders remained active after long reaction times at 1000 or 1100 °C [65]. Though these results align well with prior studies of carbon black, the advancement illustrates the coupling of the full solar spectrum, as a renewable energy form into chemical bond energy. Moreover this "solar fuel" is clean. Notably, this approach bypasses limitations of electron-hole-pair creation and separation—semiconductor limitations associated with capturing—but a fraction (near-UV) of the full solar spectrum and accomplishes catalytic conversion of solar irradiation into a clean fuel with high efficiency and catalytic longevity.

A general consensus is emerging that such carbon forms are plagued by their hallmark features; namely, porosity. The high surface area is not of benefit, as it arises from the porosity with micropores contributing the most area relative to meso or macropores. Yet surface area for carbon is but a physical metric and bears little relation to chemical catalytic reactivity. Curvature associated with pores and exposure of potential layer plane edges or other unterminated sites created during their formation may promote activity in TCD but with the inevitable result of closure by carbon deposition. First and foremost is the fact that TCD deposits carbon upon a catalyst, and the activity thereafter depends upon the structure of the deposited carbon to continue self-renewal in an autogenic manner.

2.4. Electron Microscopy in TCD

Four separate studies have shown low-resolution TEM of deposited carbon on carbon blacks [47,66–68]. Results diverge, showing either uniformity of deposition or non-uniformity, though results in both cases are difficult to gauge given varied reactor bed configurations. Three studies have examined the deposited carbon by SEM. By SEM, Shilapuram and Ozalp observed a decreasing disorder with reaction extent and temperature [61]. In the study by Nishii et al. across (activated carbon (AC), carbon black (CB), meso-porous carbon (MC) and carbon nanofiber (CNF) catalysts, examination by SEM revealed that the produced carbon was spherical in shape with a diameter of about 1 μm and covered the surface of the catalysts while sticking to each other [57]. Differently, Wang et al. (H_2 addition reference) noted formation of filamentous carbon upon their AC catalyst by SEM [56]. By these comparisons, it can be surmised that the structure of the deposited carbon may not strictly depend upon the underlying catalyst but that deposition conditions are at least equally important to directing the structure of the deposited carbon and continued self-catalytic activity.

Clearly there is disagreement with regard to catalyst structure's effects upon TCD activity, but given that analytical measures such as XRD and Raman include both original carbon and deposits, interpretation is not straightforward. As example, the deposit may replicate the initial catalyst, or its structure may diverge as deposition continues. The different initial rates of carbon deposition (or decay) reflect the dependence upon the initial catalyst structure. Differences in rates thereafter reflect a continued dependence, but with added complexities. With continuing reaction, the deposited carbon contributes while necessarily occluding the initial carbon. Surface area continues to change, but not necessarily in a monotonically increasing or decreasing way, depending upon the porosity of the underlying carbon. As illustrated in the rate plot from Suelves et al. in Figure 2, rates vary non-monotonically with time, and very different rate behaviors are observed between the different catalysts [34]. *To-date no study has examined carbon catalyst structure by HRTEM (nanostructure) for pre-characterization of the catalyst or post-characterization of the deposit. These data are crucial to identification of reactivity and assessing changes during the course of reaction.*

2.5. Results with Other Hydrocarbon Gases

Given the deactivation of the carbon catalyst with methane, an alternative solution for maintaining high catalytic activity may lie in the use of other hydrocarbons or their mixtures. Yoon et al. reported the catalytic activity of carbon black towards butane decomposition, observing no deactivation [69]. Yun et al. investigated the thermal decomposition of propane on carbon blacks, finding stable activity in a fluidized bed reactor [70]. Neither study characterized the deposit structure. In a study of mixed CH_4 and C_2H_6 , Kim et al. (2011) observed that the rate of H_2 production from CH_4 was decreased by the added C_2H_6 [71]. This was attributed to the adsorption of CH_4 on the active sites being inhibited by the more reactive intermediate C_2H_4 , resulting in a lower rate of CH_4 decomposition. However, being more reactive, C_2H_4 more than compensated for this, yielding a net increase in overall H_2 .

A more ordered structure has been related to a lower catalytic activity [21], yet results from a recent and a past study are contrary. Results from Malaika and Kozlowski show significantly higher order in the deposited carbon with methane plus propylene compared to pure methane by their XRD spectra [72] in Figure 4. However, during the course of reaction, this more ordered structure did not lead to a loss of activity. Yet XRD is a bulk measure, and therein the increased order reflects an overall average. An alternative explanation is that the pores of the activated carbon filled in, leading to an apparent increase in structure (and loss of activity), while the deposited carbon either furnished sufficient new (active) surface area and/or was sufficiently disordered so as to preserve overall activity. With surprising coincidence in our former fuel science program, 50 years ago Walker et al. studied the kinetics of propylene decomposition upon graphon, a graphitized carbon black, and found the TCD process to be 100% autocatalytic (without deactivation) [73]. Their interpretation was that the deposited carbon replicated the active surface area. Unfortunately, Malaika and Kozlowski did not measure surface area, and neither their study nor that by Walker et al. examined deposits by HRTEM to resolve these possibilities [74]. *A fundamental question raised by these studies is whether the structure and/or active sites of the deposited carbon are different than those produced by methane in TCD.*

These two observations are exciting because they suggest that a regeneration cycle may not be needed. Moreover, it should be recognized that all the reviewed studies used pure (bottled) methane. Natural gas consists of 5%–20% light hydrocarbons; i.e., it is a combination of ethane, propane and butane with balance of 80%–90% methane. Any large scale (solar) TCD process would likely use pipeline grade natural gas or even less pure natural gas (containing so-called condensable hydrocarbons) if located near an oil or gas field. Natural gas is an ever-present byproduct from oil wells, and routinely flared.

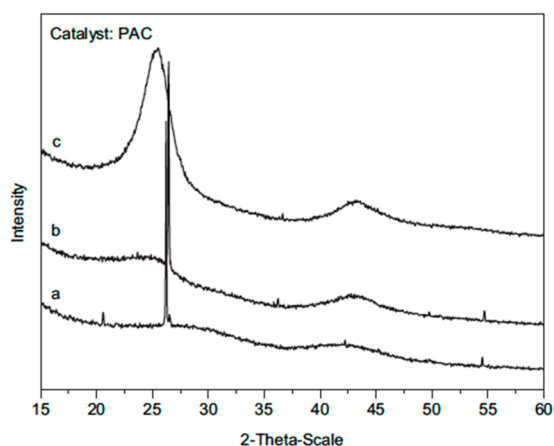


Figure 4. XRD spectra of AC samples: (a) fresh; (b) after reaction with pure methane at 850 °C; (c) after reaction with a mixture of 80% methane, 20% propylene at 850 °C [72].

2.6. CO₂ Gasification of TCD Carbon

The vast majority of TCD studies are concerned with carbon deposition and catalyst deactivation. Far fewer study regeneration of spent catalyst. Zhang et al. studied hydrogen production by carbon materials as catalysts or catalyst supports. They observed the carbon deposits from methane decomposition often had a smaller surface area and less activity than the original carbon catalyst, therein necessitating regeneration in a cyclic process [75]. Yang et al. tested the deep regeneration of activated carbon as a catalyst and performed an autothermal analysis for chemical looping methane thermo-catalytic decomposition process [76]. They reported that alone, CO₂, O₂ or H₂O could not meet the needed catalyst regeneration. Only deep regeneration using H₂O + O₂ was suitable; thereafter, the AC catalyst could maintain its physical properties. Thermodynamic modeling suggested that an autothermal process for continuous high purity H₂ could be attained.

Adamska et al. tested sequential and co-introduction of CO₂ with methane in TCD, spanning 750–950 °C and 5–50% CO₂ [77], observing increases in H₂ yield and reduction of deactivation, *but without further catalyst characterization*. Muradov [4,5] reported that the treatment of deactivated carbon samples with steam and steam–CO₂ mixtures (1:1 by volume) resulted in a significant increase in the methane decomposition rate in TCD, with the reactivated carbon *likely reflecting the large increase in porosity by the extensive burnoff*. In particular, Abbas et al. studied the CO₂ gasification of deactivated AC used in TCD, alternating decomposition with regeneration cycles, with the following results [78,79].

1. Gasification reactivity increased for higher TCD (decomposition) temperatures—rationalized by smaller crystallites (and hence more edge sites) being produced by the faster (and presumably less ordered) deposition at the higher temperatures. (This indicates that structure of deposit depends on process parameters). Moreover, this implies that temperature affects the deposition process but not the carbon once deposited.
2. With increasing (gasification) conversion, i.e., burnoff, activation energies decreased. (This suggests variation in deposit structure, with less order for the innermost portion—the earliest deposition). Notably, this is the reciprocal observation of the decline in rate with increasing deposition in nearly all studies—where the later deposit has the lowest activity and rate (attributed to higher order). That highlights the complementarity of gasification for revealing the structure of the deposited carbon. In most studies only the final deactivated catalyst is characterized, not intermediate stages. The proposed HRTEM of the deposit/catalyst at intermediate stages will address this. Atomistic simulations will co-address both deposit nanostructure evolution and its temperature dependence.

2.7. Conceptualization of Carbon Deposition in TCD and Removal via Regeneration

While the dependence upon the initial catalyst nanostructure may appear essential during initial deposition and TCD activity, as outlined by the reviewed studies, the deposited carbon rapidly covers the initial catalyst, with the subsequent deposit itself serving as catalyst. The loss of catalytic activity is not that of the original catalyst but instead reflects the declining activity of the evolving deposited carbon (for non-porous carbons such as carbon blacks). With increasing TCD duration, each incremental carbon deposit layer becomes less active than the preceding layer. Autocatalytic activity is not being maintained. To illustrate the TCD and regeneration process, Figure 5 figuratively shows the initial catalyst, carbon deposition (buildup) during TCD and regeneration, reducing the carbon deposition by oxidation (by O_2) or gasification (by CO_2 or H_2O).

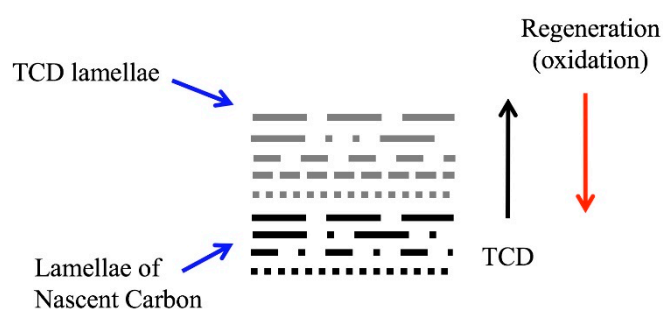


Figure 5. Illustration of deposited carbon strata (gray lines) upon the initial catalyst (solid black lines). The regeneration course through the strata is illustrated by the downward red arrow—the length of which represents the regeneration depth through the deposited carbon; it is dependent upon regeneration temperature and time, whereas TCD is denoted by the black arrow. Initial deposition may mimic/replicate the catalyst nanostructure initially, but with continued deposition the nanostructure of the deposit evolves. Regeneration, as a separate process, removes deposited carbon “layers,” with deeper levels of regeneration exposing ever earlier stages of carbon deposition and corresponding nanostructure. HRTEM is ideally suited for differentiating between the nascent carbon catalyst and carbon deposit throughout these cycles.

As Figure 5 illustrates, with increasing extent (depth) of regeneration, ever earlier carbon layers are reached, and ultimately the original catalyst is exposed and activity is (presumably) recovered. However, such recovery is short-lived, given that the initial TCD layer effectively blocks exposure of the nascent catalyst surface. Moreover, full and uniform burn-off of the deposited carbon is extremely challenging to achieve experimentally, particularly to scale without incurring substantial oxidation of the original carbon (catalyst). Uniform surface regression is not achieved simply because not all surfaces are uniformly exposed during regeneration. Finally, such catalyst recovery necessarily defeats the solid carbon capture benefits of TCD, effectively transforming methane into CO_2 .

In fact, despite the perception conveyed by Figure 5, regeneration is not merely the uncovering of an underlying carbon layer or re-exposure of an earlier stage of the deposit. Carbon mass is removed as a result of atom-by-atom oxidation or gasification (using H_2O or CO_2). As earlier stages of deposition are reached (and ultimately the original catalyst) with continued regeneration, the surface will not be as deposited, but instead possess numerous vacancies and edge and radical sites—reflecting the atomic-scale “excavation.” Such degradation of the lamellar nanostructure and the breakup of sp^2 networks therein are highly advantageous, as they account for the increase in active sites by regeneration. As such, sites become more numerous; the regeneration rate also increases. Correspondingly the TCD reactivity increases too.

The extent to which the initial carbon catalyst transfers structural similarity to the carbon deposit determines the propagation of continued activity as a first approximation. Clearly, if conditions can be controlled to form a more disordered carbon deposit featuring active sites in the form of radicals and unterminated bonds, the underlying initial carbon catalyst becomes irrelevant. For the purpose of pure

H₂, regeneration can be avoided, greatly simplifying capital hardware and operational complexity. However, if syngas generation for fuels and chemicals is desired, then regeneration becomes a beneficial requirement with deactivation, and then a trade for high, albeit temporary activity.

2.8. Economic Analyses of TCD

Various studies have considered natural gas decarbonization as a tool for greenhouse gas emission control and associated economics of TCD. Parkinson et al. examined the relative costs of carbon mitigation from a life cycle perspective for 12 different hydrogen production techniques using fossil fuels, nuclear energy and renewable sources by technology substitution [80]. Methane pyrolysis was deemed the most cost-effective short-term abatement solution, contingent upon managing its supply chain emissions and the price of solid carbon. In support, Weger et al. contends that the development of fossil-fuel decarbonization could serve as a bridging solution during the transition from a fossil-fuel based economy to a more sustainable one [81]. In an initial economic study, Keipi et al. analyzed the effect of reaction parameters on process design and the utilization possibilities of the carbon produced in TCD. Temperature and catalyst were identified as the main reaction parameters with the carbon type warranting careful consideration due to their economic impacts [82].

Considering hydrogen production, Keipi et al. subsequently conducted an economic analysis of TCD compared to steam reforming and water electrolysis [83]. They found that hydrogen production by thermal decomposition of methane would be economically competitive with steam reforming with a product carbon value of at least 280–310 EUR/tonne. By contrast, the main benefit of thermal decomposition of methane in comparison with water electrolysis is the feedstock availability via the current natural gas infrastructure, whereas electrolysis is highly dependent on the cost and availability of renewable electricity. For power generation, Abanades examined two cases to illustrate the potential application of decarbonization in the power-to-gas scenario, considering a combined cycle plant [84]. Even if hydrogen were to be cheaper due to the higher scale, the plant's efficiency reduction to 34% is only compensated by carbon taxes of between 51 and 105 EUR/ton CO₂. However, the graphitic carbon would not significantly offset costs at the industrial scale given the limited (by comparison) markets for graphitic carbon. In a detailed study of operating conditions (such as reaction temperature, reaction pressure, space velocity, feedstock purity, reactor type and material) and the catalyst characteristics (such as preparation method and conditions, catalyst type and particle size, carbon textural properties and surface chemistry) in order to facilitate hydrogen production, Zhang et al. concluded that TCD is a reliable and beneficial method for co-production of CO_x-free hydrogen and solid carbon [75]. In their review of sustainable fuel production by TCD, Srilatha et al. found that the use of carbon-based catalysts gave definite benefits over metal catalysts due to their availability, durability and low cost [85].

The extent that the initial carbon catalyst transfers structural similarity to the depositing carbon determines the propagation of continued activity as a first approximation. Clearly, if conditions can be controlled to form a more disordered carbon deposit featuring active sites in the form of radicals and unterminated bonds, the underlying initial carbon catalyst becomes irrelevant. For the purpose of pure H₂, regeneration can be avoided, greatly simplifying capital hardware and operational complexity. However, if syngas generation for fuels and chemicals is desired, then regeneration becomes a beneficial requirement with deactivation, and then a trade for high, albeit temporary activity.

3. Addressing TCD Research Needs

Knowledge gaps yet preventing sustainable TCD are summarized as follows.

1. Decline in TCD rate—and dependence upon initial catalyst and conditions.

Beyond pore filling, change in activation energy over the course of deposition and differences in activation energy between different carbons as catalysts suggest that nanostructure is changing during the course of deposition and that different carbon catalysts have initially different nanostructures.

2. Regeneration reaction conditions are yet to be mapped.

A macroscopic correlation of extent of regeneration with subsequent TCD rate and the microscopic connections with TCD active sites have yet to be made. Little is known regarding regeneration by either different oxidants (i.e., CO₂, H₂O) or as a function of temperature.

3. Connection between rates and nanostructure.

The connection between TCD rates and nanostructure is not known. No TCD study to date has evaluated nanostructure—initial or that of the deposit. These statements hold true for regeneration by H₂O and CO₂. By contrast, the dependence of “regeneration” upon nanostructure and the change in nanostructure due to “regeneration” by O₂ have received study—in the form of soot oxidation.

4. TCD Outlook

Several studies have analyzed the physical structure of the original carbon in attempting to relate activity or yield to structural aspects. Though some results suggest dependence upon the initial structure, the time-dependence of the rate cancels any further correlation. Characterization post-deposition by XRD and Raman measures both original and deposited carbon—a composite average. Changes to the original carbon structure or differences in the deposited carbon from the original are obscured. Additionally, there is a near-universal absence of testing with hydrocarbon feedstocks other than methane.

Moreover, what is the nature of active sites? It is generally accepted that the active sites on the carbon materials are where the regular array of carbon bonds is disrupted, forming free valences; discontinuities (i.e., the edges and corners of graphite crystallites); and other energetic abnormalities, such as surface defects and dislocations [58]. Hence, disordered (i.e., amorphous or microcrystalline) carbons such as carbon black and activated carbon can have a large number of active sites. However, no TCD study has related reaction rates to nanostructure or active sites. If a physical structure is changing, then, almost certainly, so is the number of active sites.

Author Contributions: R.V.W., Conceptualization, writing—original draft, writing—review and editing, supervision; M.M.N., writing—review and editing. All authors have read and agreed to the published version of the manuscript.

Funding: This research was funded by the George H. Deike, Research Endowment Fund, EMS College, Penn State is gratefully recognized.

Acknowledgments: Research support by The EMS Energy Institute is gratefully acknowledged.

Conflicts of Interest: The author declares no conflict of interest.

References

1. Abbas, H.F.; Daud, W.W. Hydrogen production by methane decomposition: A review. *Int. J. Hydrogen Energy* **2010**, *35*, 1160–1190. [CrossRef]
2. Marbán, G.; Valdés-Solís, T. Towards the hydrogen economy? *Int. J. Hydrogen Energy* **2007**, *32*, 1625–1637. [CrossRef]
3. Spath, P.L.; Mann, M.K. *Life Cycle Assessment of Hydrogen Production via Natural Gas Steam Reforming*; Technical Report NREL/TP-570-27637; National Renewable Energy Lab: Golden, CO, USA, February 2001. Available online: <https://www.osti.gov/biblio/764485> (accessed on 10 April 2020).
4. Muradov, N. Hydrogen via methane decomposition: An application for decarbonization of fossil fuels. *Int. J. Hydrogen Energy* **2001**, *26*, 1165–1175. [CrossRef]
5. Muradov, N. Thermocatalytic CO₂-free production of hydrogen from hydrocarbon fuels. In *Proceedings of the 2000 Hydrogen Program Review, NREL/CP-570-28890*; May 2000. Available online: <https://www.nrel.gov/docs/fy01osti/28890.pdf> (accessed on 10 April 2020).
6. Ahmed, S.; Aitani, A.; Rahman, F.; Al-Dawood, A.; Al-Muhaish, F. Decomposition of hydrocarbons to hydrogen and carbon. *Appl. Catal. A Gen.* **2009**, *359*, 1–24. [CrossRef]

7. Steinfeld, A. Solar thermochemical production of hydrogen—A review. *Sol. Energy* **2005**, *78*, 603–615. [[CrossRef](#)]
8. Abanades, S.; Flamant, G. Experimental study and modeling of a high-temperature solar chemical reactor for hydrogen production from methane cracking. *Int. J. Hydrogen Energy* **2007**, *32*, 1508–1515. [[CrossRef](#)]
9. Amin, A.M.; Croiset, E.; Epling, W. Review of methane catalytic cracking for hydrogen production. *Int. J. Hydrogen Energy* **2011**, *36*, 2904–2935. [[CrossRef](#)]
10. Dufour, J.; Serrano, D.P.; Galvez, J.L.; Moreno, J.; Garcia, C. Life cycle assessment of processes for hydrogen production. Environmental feasibility and reduction of greenhouse gases emissions. *Int. J. Hydrogen Energy* **2009**, *34*, 1370–1376. [[CrossRef](#)]
11. Lane, J.M.; Spath, P.L. *Technoeconomic Analysis of the Thermocatalytic Decomposition of Natural Gas*; Department of Energy: Golden, CO, USA, 2001.
12. Steinberg, M. Fossil fuel decarbonization technology for mitigating global warming. *Int. J. Hydrogen Energy* **1999**, *24*, 771–777. [[CrossRef](#)]
13. Ashik, U.P.M.; Daud, W.W.; Abbas, H.F. Production of greenhouse gas free hydrogen by thermocatalytic decomposition of methane—a review. *Renew. Sustain. Energy Rev.* **2015**, *44*, 221–256. [[CrossRef](#)]
14. Gaudernack, B.; Lynam, S. Hydrogen from natural gas without release of CO₂ to the atmosphere. *Int. J. Hydrogen Energy* **1998**, *23*, 1087–1093. [[CrossRef](#)]
15. Srilatha, K.; Viditha, V.; Srinivasulu, D.; Ramakrishna, S.U.B.; Himabindu, V. Hydrogen production using thermocatalytic decomposition of methane on Ni30/activated carbon and Ni30/carbon black. *Environ. Sci. Pollut. Res.* **2016**, *23*, 9303–9311. [[CrossRef](#)] [[PubMed](#)]
16. Rahman, M.S.; Croiset, E.; Hudgins, R.R. Catalytic decomposition of methane for hydrogen production. *Top. Catal.* **2006**, *37*, 137–145. [[CrossRef](#)]
17. De Falco, M.; Basile, A. *Enriched Methane: The First Step Towards the Hydrogen Economy*; Springer: Switzerland, 2015.
18. Aiello, R.; Fiscus, J.E.; zur Loye, H.C.; Amiridis, M.D. Hydrogen production via the direct cracking of methane over Ni/SiO₂: Catalyst deactivation and regeneration. *Appl. Catal. A Gen.* **2000**, *192*, 227–234. [[CrossRef](#)]
19. Bai, Z.; Chen, H.; Li, B.; Li, W. Catalytic decomposition of methane over activated carbon. *J. Anal. Appl. Pyrolysis* **2005**, *73*, 335–341. [[CrossRef](#)]
20. Lee, K.K.; Han, G.Y.; Yoon, K.J.; Lee, B.K. Thermocatalytic hydrogen production from the methane in a fluidized bed with activated carbon catalyst. *Catal. Today* **2004**, *93*, 81–86. [[CrossRef](#)]
21. Muradov, N.; Smith, F.; Ali, T. Catalytic activity of carbons for methane decomposition reaction. *Catal. Today* **2005**, *102*, 225–233. [[CrossRef](#)]
22. Jung, J.U.; Nam, W.; Yoon, K.J.; Han, G.Y. Hydrogen production by catalytic decomposition of methane over carbon catalysts in a fluidized bed. *Korean J. Chem. Eng.* **2007**, *24*, 674–678. [[CrossRef](#)]
23. Dunker, A.M.; Kumar, S.; Mulawa, P.A. Production of hydrogen by thermal decomposition of methane in a fluidized-bed reactor—Effects of catalyst, temperature, and residence time. *Int. J. Hydrogen Energy* **2006**, *31*, 473–484. [[CrossRef](#)]
24. Abbas, H.F.; Daud, W.W. Hydrogen production by thermocatalytic decomposition of methane using a fixed bed activated carbon in a pilot scale unit: Apparent kinetic, deactivation and diffusional limitation studies. *Int. J. Hydrogen Energy* **2010**, *35*, 12268–12276. [[CrossRef](#)]
25. Abbas, H.F.; Daud, W.W. Thermocatalytic decomposition of methane using palm shell based activated carbon: Kinetic and deactivation studies. *Fuel Process. Technol.* **2009**, *90*, 1167–1174. [[CrossRef](#)]
26. Kim, M.H.; Lee, E.K.; Jun, J.H.; Han, G.Y.; Kong, S.J.; Lee, B.K.; Yoon, K.J. Hydrogen production by catalytic decomposition of methane over activated carbons: Deactivation study. *Korean J. Chem. Eng.* **2003**, *20*, 835–839. [[CrossRef](#)]
27. Kim, M.H.; Lee, E.K.; Jun, J.H.; Kong, S.J.; Han, G.Y.; Lee, B.K.; Yoon, K.J. Hydrogen production by catalytic decomposition of methane over activated carbons: Kinetic study. *Int. J. Hydrogen Energy* **2004**, *29*, 187–193. [[CrossRef](#)]
28. Moliner, R.; Suelves, I.; Lázaro, M.J.; Moreno, O. Thermocatalytic decomposition of methane over activated carbons: Influence of textural properties and surface chemistry. *Int. J. Hydrogen Energy* **2005**, *30*, 293–300. [[CrossRef](#)]

29. Ashok, J.; Kumar, S.N.; Venugopal, A.; Kumari, V.D.; Tripathi, S.; Subrahmanyam, M. CO_x free hydrogen by methane decomposition over activated carbons. *Catal. Commun.* **2008**, *9*, 164–169. [[CrossRef](#)]
30. Lee, E.K.; Lee, S.Y.; Han, G.Y.; Lee, B.K.; Lee, T.J.; Jun, J.H.; Yoon, K.J. Catalytic decomposition of methane over carbon blacks for CO₂-free hydrogen production. *Carbon* **2004**, *42*, 2641–2648. [[CrossRef](#)]
31. Ryu, B.H.; Lee, S.Y.; Lee, D.H.; Han, G.Y.; Lee, T.J.; Yoon, K.J. Catalytic characteristics of various rubber-reinforcing carbon blacks in decomposition of methane for hydrogen production. *Catal. Today* **2007**, *123*, 303–309. [[CrossRef](#)]
32. Suelves, I.; Lázaro, M.J.; Moliner, R.; Pinilla, J.L.; Cubero, H. Hydrogen production by methane decarbonization: Carbonaceous catalysts. *Int. J. Hydrogen Energy* **2007**, *32*, 3320–3326. [[CrossRef](#)]
33. Pinilla, J.L.; Suelves, I.; Lázaro, M.J.; Moliner, R. Kinetic study of the thermal decomposition of methane using carbonaceous catalysts. *Chem. Eng. J.* **2008**, *138*, 301–306. [[CrossRef](#)]
34. Suelves, I.; Pinilla, J.L.; Lázaro, M.J.; Moliner, R. Carbonaceous materials as catalysts for decomposition of methane. *Chem. Eng. J.* **2008**, *140*, 432–438. [[CrossRef](#)]
35. Bai, Z.; Chen, H.; Li, W.; Li, B. Hydrogen production by methane decomposition over coal char. *Int. J. Hydrogen Energy* **2006**, *31*, 899–905. [[CrossRef](#)]
36. Sun, Z.Q.; Wu, J.H.; Haghighi, M.; Bromly, J.; Ng, E.; Wee, H.L.; Zhang, D.K. Methane cracking over a bituminous coal char. *Energy Fuels* **2007**, *21*, 1601–1605. [[CrossRef](#)]
37. Lázaro, M.J.; Pinilla, J.L.; Suelves, I.; Moliner, R. Study of the deactivation mechanism of carbon blacks used in methane decomposition. *Int. J. Hydrogen Energy* **2008**, *33*, 4104–4111. [[CrossRef](#)]
38. Muradov, N. Thermocatalytic CO₂-Free Production of Hydrogen from Hydrocarbon Fuels; U.S. DOE Hydrogen Program Review. U.S.: Department of Energy (DOE); 2002; NREL/CP-610-32405. Available online: <https://www.nrel.gov/docs/fy02osti/32405a17.pdf> (accessed on 10 April 2020).
39. Bai, Z.; Li, W.; Bai, J.; Li, B.; Chen, H. The effects of textural properties and surface chemistry of activated carbon on its catalytic performance in methane decomposition for hydrogen production. *Energy Sources Part A Recovery Util. Environ. Eff.* **2012**, *34*, 1145–1153. [[CrossRef](#)]
40. Pinilla, J.L.; Suelves, I.; Lázaro, M.J.; Moliner, R. Influence on hydrogen production of the minor components of natural gas during its decomposition using carbonaceous catalysts. *J. Power Sources* **2009**, *192*, 100–106. [[CrossRef](#)]
41. Muradov, N.; Smith, F.; Bokerman, G. Methane activation by nonthermal plasma generated carbon aerosols. *J. Phys. Chem. C* **2009**, *113*, 9737–9747. [[CrossRef](#)]
42. Moliner, R.; Suelves, I.; Lázaro, M.J.; Corbella, B.M.; Palacios, J.M. Hydrogen production by catalytic decomposition of methane over carbonaceous materials. In Proceedings of the International Conference on Carbon, Oviedo, Spain, 6–10 July 2003.
43. Pinilla, J.L.; Suelves, I.; Utrilla, R.; Gálvez, M.E.; Lázaro, M.J.; Moliner, R. Hydrogen production by thermo-catalytic decomposition of methane: Regeneration of active carbons using CO₂. *J. Power Sources* **2007**, *169*, 103–109. [[CrossRef](#)]
44. Serrano, D.P.; Botas, J.A.; Guil-Lopez, R. H₂ production from methane pyrolysis over commercial carbon catalysts: Kinetic and deactivation study. *Int. J. Hydrogen Energy* **2009**, *34*, 4488–4494. [[CrossRef](#)]
45. Serrano, D.P.; Botas, J.A.; Fierro, J.L.G.; Guil-López, R.; Pizarro, P.; Gómez, G. Hydrogen production by methane decomposition: Origin of the catalytic activity of carbon materials. *Fuel* **2010**, *89*, 1241–1248. [[CrossRef](#)]
46. Krzyżyński, S.; Kozłowski, M. Activated carbons as catalysts for hydrogen production via methane decomposition. *Int. J. Hydrogen Energy* **2008**, *33*, 6172–6177. [[CrossRef](#)]
47. Lee, S.Y.; Ryu, B.H.; Han, G.Y.; Lee, T.J.; Yoon, K.J. Catalytic characteristics of specialty carbon blacks in decomposition of methane for hydrogen production. *Carbon* **2008**, *46*, 1978–1986. [[CrossRef](#)]
48. Malaika, A.; Kozłowski, M. Influence of ethylene on carbon-catalysed decomposition of methane. *Int. J. Hydrogen Energy* **2009**, *34*, 2600–2605. [[CrossRef](#)]
49. Kameya, Y.; Hanamura, K. Carbon black texture evolution during catalytic methane decomposition. *Carbon* **2012**, *50*, 3503–3512. [[CrossRef](#)]
50. Müller, J.O.; Su, D.S.; Jentoft, R.E.; Kröhnert, J.; Jentoft, F.C.; Schlögl, R. Morphology-controlled reactivity of carbonaceous materials towards oxidation. *Catal. Today* **2005**, *102*, 259–265. [[CrossRef](#)]
51. Song, J.; Alam, M.; Boehman, A.L.; Kim, U. Examination of the oxidation behavior of biodiesel soot. *Combust. Flame* **2006**, *146*, 589–604. [[CrossRef](#)]

52. Al-Qurashi, K.; Boehman, A.L. Impact of exhaust gas recirculation (EGR) on the oxidative reactivity of diesel engine soot. *Combust. Flame* **2008**, *155*, 675–695. [[CrossRef](#)]
53. Knauer, M.; Schuster, M.E.; Su, D.; Schlögl, R.; Niessner, R.; Ivleva, N.P. Soot structure and reactivity analysis by Raman microspectroscopy, temperature-programmed oxidation, and high-resolution transmission electron microscopy. *J. Phys. Chem. A* **2009**, *113*, 13871–13880. [[CrossRef](#)]
54. Liu, F.; Yang, L.; Song, C. Chemical looping hydrogen production using activated carbon and carbon black as multi-function carriers. *Int. J. Hydrogen Energy* **2018**, *43*, 5501–5511. [[CrossRef](#)]
55. Mahmoudi, M.; Dentzer, J.; Gadiou, R.; Ouederni, A. Evaluation of activated carbons based on olive stones as catalysts during hydrogen production by thermocatalytic decomposition of methane. *Int. J. Hydrogen Energy* **2017**, *42*, 8712–8720. [[CrossRef](#)]
56. Wang, J.; Jin, L.; Zhou, Y.; Li, Y.; Hu, H. Effect of Ca (NO₃)₂ addition in coal on properties of activated carbon for methane decomposition to hydrogen. *Fuel Process. Technol.* **2018**, *176*, 85–90. [[CrossRef](#)]
57. Nishii, H.; Miyamoto, D.; Umeda, Y.; Hamaguchi, H.; Suzuki, M.; Tanimoto, T.; Harigai, T.; Takikawa, H.; Suda, Y. Catalytic activity of several carbons with different structures for methane decomposition and by-produced carbons. *Appl. Surf. Sci.* **2019**, *473*, 291–297. [[CrossRef](#)]
58. Więckowski, A.B.; Najder-Kozdrowska, L.; Rechnia, P.; Malaika, A.; Krzyżyńska, B.; Kozłowski, M. EPR Characteristics of Activated Carbon for Hydrogen Production by the Thermo-Catalytic Decomposition of Methane. *Acta Phys. Pol. A* **2016**, *130*, 701–704. [[CrossRef](#)]
59. Ghani, S.A.; Al Saraj, M.A.A.; Razaq, G.A. Catalytic Production of CO_x Free Hydrogen by Methane Decomposition over Activated Carbons. *Energy Sources Part A Recovery Util. Environ. Eff.* **2015**, *37*, 326–333. [[CrossRef](#)]
60. Shen, Y.; Lua, A.C. A trimodal porous carbon as an effective catalyst for hydrogen production by methane decomposition. *J. Colloid Interface Sci.* **2016**, *462*, 48–55. [[CrossRef](#)] [[PubMed](#)]
61. Shilapuram, V.; Ozalp, N. Hydrogen production by carbon-catalyzed methane decomposition via thermogravimetry. *J. Energy Resour. Technol.* **2017**, *139*, 012005. [[CrossRef](#)]
62. Luo, H.; Qiao, Y.; Ning, Z.; Bo, C.; Hu, J. Effect of Thermal Extraction on Coal-Based Activated Carbon for Methane Decomposition to Hydrogen. *ACS Omega* **2020**, *5*, 2465–2472. [[CrossRef](#)]
63. Wang, J.; Jin, L.; Li, Y.; Wang, M.; Hu, H. Effect of hydrogen additive on methane decomposition to hydrogen and carbon over activated carbon catalyst. *Int. J. Hydrogen Energy* **2018**, *43*, 17611–17619. [[CrossRef](#)]
64. Gadkari, S.; Fidalgo, B.; Gu, S. Numerical analysis of microwave assisted thermocatalytic decomposition of methane. *Int. J. Hydrogen Energy* **2017**, *42*, 4061–4068. [[CrossRef](#)]
65. Abanades, S.; Kimura, H.; Otsuka, H. Kinetic investigation of carbon-catalyzed methane decomposition in a thermogravimetric solar reactor. *Int. J. Hydrogen Energy* **2015**, *40*, 10744–10755. [[CrossRef](#)]
66. Kameya, Y.; Hanamura, K. Variation in catalytic activity of carbon black during methane decomposition: Active site estimations from surface structural characteristics. *Catal. Lett.* **2012**, *142*, 460–463. [[CrossRef](#)]
67. Lee, S.C.; Seo, H.J.; Han, G.Y. Hydrogen production by catalytic decomposition of methane over carbon black catalyst at high temperatures. *Korean J. Chem. Eng.* **2013**, *30*, 1716–1721. [[CrossRef](#)]
68. Kameya, Y.; Hanamura, K. Kinetic and Raman spectroscopic study on catalytic characteristics of carbon blacks in methane decomposition. *Chem. Eng. J.* **2011**, *173*, 627–635. [[CrossRef](#)]
69. Yoon, S.H.; Park, N.K.; Lee, T.J.; Yoon, K.J.; Han, G.Y. Hydrogen production by thermocatalytic decomposition of butane over a carbon black catalyst. *Catal. Today* **2009**, *146*, 202–208. [[CrossRef](#)]
70. Yun, Y.H.; Lee, S.C.; Jang, J.T.; Yoon, K.J.; Bae, J.W.; Han, G.Y. Thermo-catalytic decomposition of propane over carbon black in a fluidized bed for hydrogen production. *Int. J. Hydrogen Energy* **2014**, *39*, 14800–14807. [[CrossRef](#)]
71. Kim, M.S.; Lee, S.Y.; Kwak, J.H.; Han, G.Y.; Yoon, K.J. Hydrogen production by decomposition of ethane-containing methane over carbon black catalysts. *Korean J. Chem. Eng.* **2011**, *28*, 1833–1838. [[CrossRef](#)]
72. Malaika, A.; Kozłowski, M. Hydrogen production by propylene-assisted decomposition of methane over activated carbon catalysts. *Int. J. Hydrogen Energy* **2010**, *35*, 10302–10310. [[CrossRef](#)]
73. Hoffman, W.P.; Vastola, F.J.; Walker, P.L. Pyrolysis of propylene over carbon active sites—I: Kinetics. *Carbon* **1985**, *23*, 151–161. [[CrossRef](#)]
74. Walker, P.L. Carbon: An old but new material revisited. *Carbon* **1990**, *28*, 261–279. [[CrossRef](#)]

75. Zhang, J.; Li, X.; Chen, H.; Qi, M.; Zhang, G.; Hu, H.; Ma, X. Hydrogen production by catalytic methane decomposition: Carbon materials as catalysts or catalyst supports. *Int. J. Hydrogen Energy* **2017**, *42*, 19755–19775. [[CrossRef](#)]
76. Yang, L.; Liu, F.; Liu, Y.; Quan, W.; He, J. Deep regeneration of activated carbon catalyst and autothermal analysis for chemical looping methane thermo-catalytic decomposition process. *Int. J. Hydrogen Energy* **2018**, *43*, 17633–17642. [[CrossRef](#)]
77. Adamska, A.; Malaika, A.; Kozłowski, M. Carbon-catalyzed decomposition of methane in the presence of carbon dioxide. *Energy Fuels* **2010**, *24*, 3307–3312. [[CrossRef](#)]
78. Abbas, H.F.; Daud, W.W. An experimental investigation into the CO₂ gasification of deactivated activated-carbon catalyst used for methane decomposition to produce hydrogen. *Int. J. Hydrogen Energy* **2010**, *35*, 141–150. [[CrossRef](#)]
79. Abbas, H.F.; Daud, W.W. Thermocatalytic decomposition of methane for hydrogen production using activated carbon catalyst: Regeneration and characterization studies. *Int. J. Hydrogen Energy* **2009**, *34*, 8034–8045. [[CrossRef](#)]
80. Parkinson, B.; Balcombe, P.; Speirs, J.F.; Hawkes, A.D.; Hellgardt, K. Levelized cost of CO₂ mitigation from hydrogen production routes. *Energy Environ. Sci.* **2019**, *12*, 19–40. [[CrossRef](#)]
81. Weger, L.; Abánades, A.; Butler, T. Methane cracking as a bridge technology to the hydrogen economy. *Int. J. Hydrogen Energy* **2017**, *42*, 720–731. [[CrossRef](#)]
82. Keipi, T.; Tolvanen, K.E.; Tolvanen, H.; Konttinen, J. Thermo-catalytic decomposition of methane: The effect of reaction parameters on process design and the utilization possibilities of the produced carbon. *Energy Convers. Manag.* **2016**, *126*, 923–934. [[CrossRef](#)]
83. Keipi, T.; Tolvanen, H.; Konttinen, J. Economic analysis of hydrogen production by methane thermal decomposition: Comparison to competing technologies. *Energy Convers. Manag.* **2018**, *159*, 264–273. [[CrossRef](#)]
84. Abánades, A. Natural gas decarbonization as tool for Greenhouse Gases Emission Control. *Front. Energy Res.* **2018**, *6*, 47. [[CrossRef](#)]
85. Srilatha, K.; Bhagawan, D.; Kumar, S.S.; Himabindu, V. Sustainable fuel production by thermocatalytic decomposition of methane—A review. *S. Afr. J. Chem. Eng.* **2017**, *24*, 156–167. [[CrossRef](#)]



© 2020 by the authors. Licensee MDPI, Basel, Switzerland. This article is an open access article distributed under the terms and conditions of the Creative Commons Attribution (CC BY) license (<http://creativecommons.org/licenses/by/4.0/>).